Eur. Phys. J. D **19**, 411–419 (2002)
DOI: 10.1140/epjd/e20020079

THE EUROPEAN PHYSICAL JOURNAL D
EDP Sciences

Absorption and dispersion by a multiple driven two-level atom

Z. Ficek[1,2,a], J. Seke[1], A.V. Soldatov[1,3], G. Adam[1], and N.N. Bogolubov Jr[1,3]

[1] Institut für Theoretische Physik, Technische Universität Wien, Wiedner Hauptstrasse 8-10/136, 1040 Wien, Austria
[2] Department of Physics and Centre for Laser Science, The University of Queensland, Brisbane, QLD 4072, Australia
[3] Department of Statistical Mechanics, V.A. Steklov Mathematical Institute, GSP-1, 117966, Gubkin Street 8, Moscow, Russia

Received 23 October 2001 and Received in final form 31 January 2002

Abstract. We investigate the absorption and dispersion properties of a two-level atom driven by a polychromatic field. The driving field is composed of a strong resonant (carrier) frequency component and a large number of symmetrically detuned sideband fields (modulators). A rapid increase in the absorption at the central frequency and the collapse of the response of the system from multiple frequencies to a single frequency are predicted to occur when the Rabi frequency of the modulating fields is equal to the Rabi frequency of the carrier field. These are manifestations of the undressing or a disentanglement of the atomic and driving field states, that leads to a collapse of the atom to its ground state. Our calculation permits consideration of the question of the undressing of the driven atom by a multiple-modulated field and the predicted spectra offer a method of observing undressing. Moreover, we find that the absorption and dispersion spectra split into multiplets whose structures depend on the Rabi frequency of the modulating fields. The spectral features can jump between different resonance frequencies by changing the Rabi frequency of the modulating fields or their initial phases, which can have potential applications as a quantum frequency filter.

PACS. 32.50.+d Fluorescence, phosphorescence (including quenching) – 32.80.-t Photon interactions with atoms – 32.80.Qk Coherent control of atomic interactions with photons – 42.50.Gy Effects of atomic coherence on propagation, absorption, and amplification of light – 42.50.Ar Photon statistics and coherence theory

1 Introduction

The study of coherent effects in resonant media has recently attracted a great deal of interest, especially due to the prediction [1] and experimental observation [2] of a steep anomalous and normal dispersion accompanied by electromagnetically induced transparency [3]. The dispersion of radiation by matter is certainly one of the fundamental physical properties. The usual dispersion-absorption relations tell us that at frequencies at which the dispersion is large and steep, absorption by the medium is also large. For example, in an undriven atom the dispersion is large near the transition frequency, but at this frequency the absorption is very high as well, and therefore an incident probe field would be absorbed within a distance of the order of the transition wavelength. It has been shown that an application of a strong driving field could change the absorptive and dispersive properties of two-level [4] and multi-level atoms [5] such that a high dispersion can be achieved accompanied by vanishing absorption.

In the case of driven atoms the absorption is a balance between stimulated absorption and emission, which causes the cancellation of the absorptive features corresponding to transitions between equally populated levels [6]. While the main interest in the absorption and dispersion of optical materials has been focused on the case of a weak probing field [7], the driven two-level atom with an arbitrary strong probe intensity has also been investigated in the context of a search for nonlinear effects in the atom-field interaction [8]. The results showed that the strongly probed system can response not only at harmonics, but also at subharmonics of the Rabi frequency of the driving field [9]. The resonances correspond to multi-photon absorption by the driven atom, and the physical origin of these features is explained by the dressed-atom model [10].

Recently, we developed a theory of the fluorescence spectrum of a two-level atom driven by a multiple modulated field [11]. We assumed that the modulated field is composed of a strong resonant frequency component and a large number of symmetrically detuned sideband fields displaced from the central component by integer multiples of a constant detuning. We found that two distinctly different types of the fluorescence spectra can be observed depending on the Rabi frequency of the modulating fields

[a] e-mail: ficek@physics.uq.edu.au

and their initial phase relative to the phase of the strong central component. For equal relative phases, the effective Rabi frequency of the driving field reduces to zero resulting in the disappearance of the fluorescence spectrum. On the other hand, for the opposite relative phases, the spectrum exhibits a triplet structure with the sidebands located at frequencies equal to the sum of the Rabi frequencies of the field components. It should be noted that a multiple modulated field could be realised experimentally by applying a multi-mode symmetric mode-locked laser [12], or by applying electro-optic modulator of a single-mode laser [13].

It is the purpose of this paper to study the absorption and dispersion properties of a two-level atom driven by a multiple modulated field. Comparison is made with the absorption and dispersion spectra calculated for a monochromatic driving field [4,6,7]. The fluorescence spectra described above lead one to suspect that the absorption and dispersion spectra arising from an atom driven by a multiple modulated field will display interesting features. Indeed, we find that the spectra differ qualitatively from those found for the monochromatic and bichromatic driving fields. In particular, we exploit the fact that the absorptive and dispersive properties of a two-level atom can be dramatically modified by controlling the amplitude and phase of the sideband components of a polychromatic driving field. Moreover, we show that a multiple modulation can lead to an amplification of the probe field at frequencies that are independent of the Rabi frequency of the driving field. The amplification features can jump between different resonance frequencies by changing the Rabi frequency of the modulating fields or their initial phases, which could allow to filter signals of well defined frequencies.

2 Absorption and dispersion of a probe beam

The system under investigation consists of a two-level atom driven by a coherent multi-chromatic field and damped by spontaneous emission into the remaining vacuum modes of the three-dimensional electromagnetic (EM) field. The atom has excited state $|2\rangle$, ground state $|1\rangle$, and transition frequency $\omega_{\rm a}$. The zero of energy for the atom is taken to be midway between the ground and excited states such that the ground state energy (in units of $\hbar\omega_{\rm a}$) equals to $-1/2$.

The driving field is taken as a polychromatic field composed of a large number of discrete modes of the amplitude

$$\begin{aligned}\mathbf{E}(t) &= \frac{1}{2}\sum_{n=-p}^{p}\mathbf{E}_n e^{i(\omega_n t+\psi_n)} + \text{c.c.}\\ &= \frac{1}{2}e^{i(\omega_0 t+\psi_0)}\sum_{n=-p}^{p}\mathbf{E}_n e^{i(\delta_n t+\phi_n)} + \text{c.c.},\end{aligned} \quad (1)$$

where $\mathbf{E}_n(t)$ and ω_n are the amplitude and frequency of the nth component, respectively, $\delta_n = \omega_n - \omega_0$ is the detuning between the nth sideband component ($n \neq 0$) and the carrier ($n = 0$) component of the field, $2p + 1 = N$ is the number of the field components, ψ_n is the phase of the nth component and $\phi_n = \psi_n - \psi_0$ is the relative initial ($t = 0$) phase between the carrier and the nth sideband component. Further on, for simplicity, we will set the phase of the carrier field $\psi_0 = 0$, and will assume that the frequency ω_0 of the carrier is resonant with the atomic transition frequency, *i.e.* the detuning $\Delta = \omega_{\rm a} - \omega_0$ is zero.

In the interaction picture, the master equation for the density operator of the system has the form [14]

$$\begin{aligned}\frac{\partial}{\partial t}\rho(t) &= -\frac{i}{\hbar}\left[\tilde{H},\rho(t)\right]\\ &\quad -\frac{1}{2}\Gamma\left(\tilde{S}^+\tilde{S}^-\rho(t)+\rho(t)\tilde{S}^+\tilde{S}^- - 2\tilde{S}^-\rho(t)\tilde{S}^+\right),\end{aligned} \quad (2)$$

where

$$\tilde{S}^{\pm}(t) = \pm i S^{\pm} e^{\mp i\omega_0 t} \quad (3)$$

are slowly varying parts of the atomic spin raising ($S^+ = |2\rangle\langle 1|$) and lowering ($S^- = |1\rangle\langle 2|$) operators, Γ is the spontaneous emission rate and $\tilde{H}$ is the interaction Hamiltonian of the polychromatic field with the atom, which in the electric-dipole and rotating-wave approximations is given by

$$\tilde{H} = -\frac{1}{2}i\hbar\left[\sum_{n=-p}^{p}\Omega_n e^{-i(\delta_n t+\phi_n)}S^+ - \text{H.c.}\right]. \quad (4)$$

Here, Ω_n is the Rabi frequency of the nth component of the driving field.

We proceed by writing down equations of motion for the expectation values of the atomic operators derived from the master equation (2). The equations can be written in a compact matrix form as

$$\frac{\partial}{\partial t}X(t) = \mathcal{M}(t)X(t) + L, \quad (5)$$

where $X(t)$ is a column vector with the components $X_1(t) = \text{Tr}[S^-\rho(t)] = \langle\tilde{S}^-(t)\rangle, X_2(t) = \text{Tr}[S^+\rho(t)] = \langle\tilde{S}^+(t)\rangle, X_3(t) = \text{Tr}[S^z\rho(t)] = \langle\tilde{S}^z(t)\rangle$, and $\tilde{S}^z(t) = S^z = (|2\rangle\langle 2| - |1\rangle\langle 1|)/2$ is the population inversion operator. In equation (5), $\mathcal{M}(t)$ is a complex 3×3 matrix

$$\mathcal{M}(t) = \begin{pmatrix} -\frac{1}{2}\Gamma & 0 & \Omega(t)\\ 0 & -\frac{1}{2}\Gamma & \Omega^*(t)\\ -\frac{1}{2}\Omega^*(t) & -\frac{1}{2}\Omega(t) & -\Gamma\end{pmatrix}, \quad (6)$$

with

$$\Omega(t) = \sum_{n=-p}^{p}\Omega_n \exp[-i(\delta_n t+\phi_n)], \quad (7)$$

and L is an inhomogeneous term with components $L_1 = L_2 = 0$ and $L_3 = -\Gamma/2$.

The equation (5) are the first-order differential equations with time dependent coefficients. For a large number of the components of the driving field, the coefficients

are quite complicated and in general involve N different parameters δ_n. The analytical or numerical treatment of such a problem becomes extremely difficult. However, the problem simplifies when the frequencies of the field components are equidistant and symmetrically distributed about the carrier frequency ω_0. In the following, we will explore the special case of $\delta_n = n\delta$ and $\Omega_{-n} = \Omega_n$. We will also assume that $\phi_{-n} = \phi_n$. In this special case the time dependence of $\Omega(t)$ can be expressed in terms of a single parameter δ as

$$\Omega(t) = \Omega_0 + 2\sum_{n=1}^{p} \Omega_n \mathrm{e}^{-\mathrm{i}\phi_n} \cos n\delta t. \tag{8}$$

It is seen from equation (8) that the sideband fields act as a multiple modulator of the Rabi frequency Ω_0 of the carrier component. Depending on the initial phase ϕ_n, the sideband fields can modulate the amplitude or the phase of Ω_0. For $\phi_n = 0$ or π the sidebands act as a multiple modulator of the amplitude

$$\Omega(t) = \Omega_0 \left(1 \pm \sum_{n=1}^{p} a_n \cos n\delta t\right), \tag{9}$$

where $a_n = 2\Omega_n/\Omega_0$ is the modulation amplitude and the sign "$+$" corresponds to $\phi_n = 0$, while "$-$" corresponds to $\phi_n = \pi$.

We now suppose that the system is weakly perturbed by a monochromatic probe field of a frequency ω, in whose absorption and dispersion we are interested. The probe absorption and dispersion essentially explore the atom plus driving field entangled states (dressed states) and especially their relative populations. Various components of the spectra are associated with different transition frequencies between these dressed states. In the course of previous work on absorption spectra in amplitude-modulated fields only the cases of a small number of the modulating fields, $p = 1$ and $p = 2$, have been studied [15]. Here, we treat the opposite limit of a large number of the modulating fields ($p \gg 1$). The special significance of this case is that the absorption and dispersion spectra strongly depend on the Rabi frequency and phase of the modulating fields, and also an analytical treatment can be given that clearly explains the predicted spectral features.

The linear susceptibility $\chi(\omega)$ of the probe field at frequency ω is given in terms of the Fourier transform of the average value of the two-time commutator of the atomic dipole operators as [6,16,17]

$$\chi(\omega) = \Gamma\left(\frac{1}{T}\int_0^T \mathrm{d}t' \int_0^{t'} \mathrm{d}t \langle[\tilde{S}^-(t), \tilde{S}^+(t')]\rangle \mathrm{e}^{\mathrm{i}\nu(t-t')}\right), \tag{10}$$

where T is the integrating time of the detector, and $\nu = \omega - \omega_0$.

Invoking the quantum regression theorem [18] together with the equations of motion (5), one may obtain equations of motion for the two-time correlation functions $\langle[\tilde{S}^-(t), \tilde{S}^+(t')]\rangle$, $\langle[\tilde{S}^+(t), \tilde{S}^+(t')]\rangle$ and $\langle[\tilde{S}^z(t), \tilde{S}^+(t')]\rangle$. The equations are formally the same as equation (5), but with

$$\begin{aligned} X_1(t) &\to \chi_1(t,t') = \langle[\tilde{S}^-(t), \tilde{S}^+(t')]\rangle, \\ X_2(t) &\to \chi_2(t,t') = \langle[\tilde{S}^+(t), \tilde{S}^+(t')]\rangle, \\ X_3(t) &\to \chi_3(t,t') = \langle[S^z(t), \tilde{S}^+(t')]\rangle, \end{aligned} \tag{11}$$

and the inhomogeneous term $L = 0$.

To illustrate the effect of a multiple modulation on the two-level atom, we solve equation (5) using the Floquet method [19], in which the atomic dynamics are described in terms of Fourier harmonics of the atomic variables. In this approach, we make a harmonic decomposition of the expectation values of the commutators

$$\chi_k(t,t') = \sum_{l=-\infty}^{\infty} \chi_k^{(l)}(t,t') \mathrm{e}^{\mathrm{i}l\delta t}, \qquad k = 1,2,3, \tag{12}$$

where $\chi_k^{(l)}(t,t')$ are slowly varying two-time harmonic amplitudes.

By substituting equation (12) into equation (5) and comparing coefficients of the same powers in $l\delta$, we obtain that the equations of motion for the harmonic amplitudes take the form

$$\begin{aligned} \frac{\partial}{\partial t}\chi_1^{(l)} &= -\left(\frac{1}{2}\Gamma + \mathrm{i}l\delta\right)\chi_1^{(l)} + \sum_{n=-p}^{p} \tilde{\Omega}_n \chi_3^{(l+n)}, \\ \frac{\partial}{\partial t}\chi_2^{(l)} &= -\left(\frac{1}{2}\Gamma + \mathrm{i}l\delta\right)\chi_2^{(l)} + \sum_{n=-p}^{p} \tilde{\Omega}_n^* \chi_3^{(l-n)}, \\ \frac{\partial}{\partial t}\chi_3^{(l)} &= -(\Gamma + \mathrm{i}l\delta)\chi_3^{(l)} - \frac{1}{2}\sum_{n=-p}^{p} \tilde{\Omega}_n^* \chi_1^{(l-n)} \\ &\quad -\frac{1}{2}\sum_{n=-p}^{p} \tilde{\Omega}_n \chi_2^{(l+n)}. \end{aligned} \tag{13}$$

Taking the Laplace transform of equation (13) over the time variable $\tau = t - t'$ and eliminating $\chi_1^{(l)}(z)$ and $\chi_2^{(l)}(z)$, the set of equations (13) can be written in a form of an inhomogeneous $(2N-1)$-term recurrence relation for $\chi_3^{(l)}(z)$ as

$$\begin{aligned} (z + \Gamma + \mathrm{i}l\delta)\chi_3^{(l)}(z) &+ \frac{1}{2}\sum_n \sum_m \frac{\tilde{\Omega}_n^* \tilde{\Omega}_m}{P_{l-n}(z)} \chi_3^{(l-n+m)}(z) \\ &+ \frac{1}{2}\sum_n \sum_m \frac{\tilde{\Omega}_n \tilde{\Omega}_m^*}{P_{l+n}(z)} \chi_3^{(l+n-m)}(z) \\ &= g_l(z), \end{aligned} \tag{14}$$

where $P_l(z) = z + (1/2)\Gamma + \mathrm{i}l\delta$, z is a complex (Laplace transform) parameter, and

$$\begin{aligned} g_l(z) = \chi_3^{(l)}(t',t') &- \frac{1}{2}\sum_n \frac{\tilde{\Omega}_n^*}{P_{l-n}(z)} \chi_1^{(l-n)}(t',t') \\ &- \frac{1}{2}\sum_n \frac{\tilde{\Omega}_n}{P_{l+n}(z)} \chi_2^{(l+n)}(t',t') \end{aligned} \tag{15}$$

is an inhomogeneous term given by the initial values $(t = t')$ of the atomic correlation functions

$$\chi_1^{(l)}(t',t') = -2X_3^{(l)}(t'),$$
$$\chi_2^{(l)}(t',t') = 0,$$
$$\chi_3^{(l)}(t',t') = X_2^{(l)}(t'). \quad (16)$$

In equation (16), $X_k^{(l)}(t')$ are the stationary harmonic amplitudes of the expectation values of the atomic dipole operators, which can be found from the following recurrence relation

$$(\Gamma + il\delta) X_3^{(l)} + \frac{1}{2}\sum_{m,n} \frac{\tilde{\Omega}_m \tilde{\Omega}_n^*}{P_{l-n}} X_3^{(l-n+m)} + \frac{1}{2}\sum_{m,n} \frac{\tilde{\Omega}_m^* \tilde{\Omega}_n}{P_{l+n}} X_3^{(l+n-m)} = -\frac{1}{2}\Gamma\delta_{l,0}, \quad (17)$$

where $P_l = (1/2)\Gamma + il\delta$, $\tilde{\Omega}_n = \Omega_n \exp(-i\phi_n)$, and $\delta_{l,0}$ is the Kronecker delta function.

The linear susceptibility (10) can be written as

$$\chi(\omega) = \chi'(\omega) + i\chi''(\omega), \quad (18)$$

where the real (χ') and imaginary (χ'') parts of χ determine the absorption and dispersion spectra of the probe field. According to equations (10, 11), the stationary probe absorption and dispersion spectra are given, respectively, by the real and imaginary parts of the zeroth-order harmonic $\chi_1^{(0)}(z)$ as

$$\chi'(\omega) = \Gamma \mathrm{Re}\chi_1^{(0)}(z)|_{z=-i\nu}, \quad (19)$$

and

$$\chi''(\omega) = \Gamma \mathrm{Im}\chi_1^{(0)}(z)|_{z=-i\nu}, \quad (20)$$

where

$$\chi_1^{(0)}(z) = \frac{1}{P_0(z)}\left(-2X_3^{(0)}(t',t') + \sum_{n=-p}^{p} \tilde{\Omega}_n \chi_3^{(n)}(z)\right). \quad (21)$$

The expression (21) is our formal result for the absorption and dispersion spectra of a two-level atom driven by a multiple amplitude-modulated field. The first term of equation (21) involves the stationary component of the population inversion between the atomic levels, whereas the second term involves the quantities $\chi_3^{(n)}(z)$ which are found from the recurrence relation (18) by using a truncated basis of the harmonic amplitudes and a numerical continued fraction technique [19]. Thus, using the result (21), the weak probe field absorption and dispersion spectra can be evaluated to any desired accuracy and for an arbitrary number of modulating fields. The susceptibility (21) is a function of the detuning δ, the Rabi frequency Ω_n and the phase ϕ_n. For fixed Ω_0 and δ, one can observe absorption and dispersion spectra as a function of

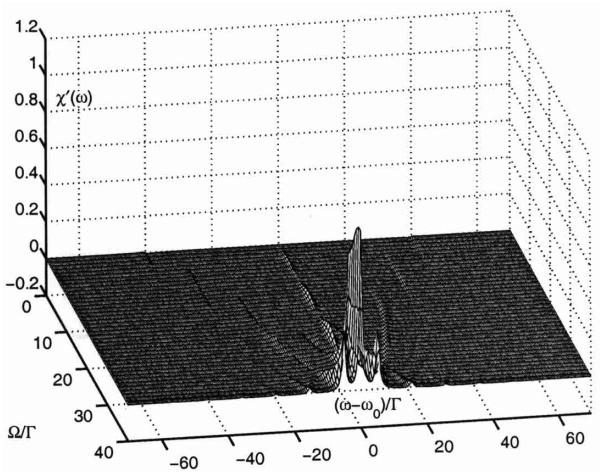

Fig. 1. Three-dimensional absorption spectra $\chi'(\omega)$ as a function of $(\omega - \omega_0)/\Gamma$ and Ω/Γ for $\Omega_0 = 40\Gamma, \delta = 10\Gamma, p = 25$, and $\phi_n = 0$.

ν and the Rabi frequency $\Omega_{n\neq 0} = \Omega$ of the modulating fields. In the following, we give illustrative figures of the dependence of the absorption and dispersion spectra on Ω and ϕ_n.

In Figure 1, we present the three-dimensional absorption spectrum $\chi'(\omega)$ for $\Omega_0 = 40\Gamma, \delta = 10\Gamma, p = 25$, and $\phi_n = 0$. The graph shows how the absorption spectrum is modified when the Rabi frequency of the modulating fields varies. In the absence of the modulating fields, $\Omega = 0$, and then the spectrum exhibits the familiar Mollow absorption spectrum [6] with very small dispersive structures at $\nu = \pm\Omega_0$ and vanishing absorption (transparency) at $\nu = 0$. When the Rabi frequency of the modulating fields increases, an absorption peak emerges at $\nu = 0$. As Ω increases further, the amplitude of the peak increases in an oscillatory manner and the small dispersive structures move towards the central peak. As it is shown in Section 3, the oscillations of the amplitude of the central peak result from the oscillations of the population inversion between the atomic bare states. For $\Omega < \Omega_0$ the amplitude of the oscillations is small and slowly increases with Ω. When $\Omega \simeq \Omega_0$, the dominant feature of the spectrum is a large absorptive peak at the central frequency. Thus, the modulating field turns the atom into its ground state. The continuous move of the small sideband features towards the central component and the appearance of a strong absorption peak for $\Omega \simeq \Omega_0$ clearly demonstrates that atom collapses into its ground state when $\Omega = \Omega_0$. That is, for $\Omega = \Omega_0$ the atomic and driving field states completely disentangles. In other words, the effect of the modulating fields is to "undress" the atom.

The manner in which the absorption spectrum evolves with Ω is different for $\phi_n = \pi$. This is shown in Figure 2, where we plot the spectrum for the same parameters as in Figure 1, but $\Omega \to -\Omega$. Again, the sideband features remain dispersive independent of Ω. As Ω increases the dispersive features jump towards larger resonance frequencies and their amplitudes attain maxima when $\Omega = n\delta$, where $n = 0, 1, 2, \ldots$ The central peak, suppressed at $\Omega = 0$,

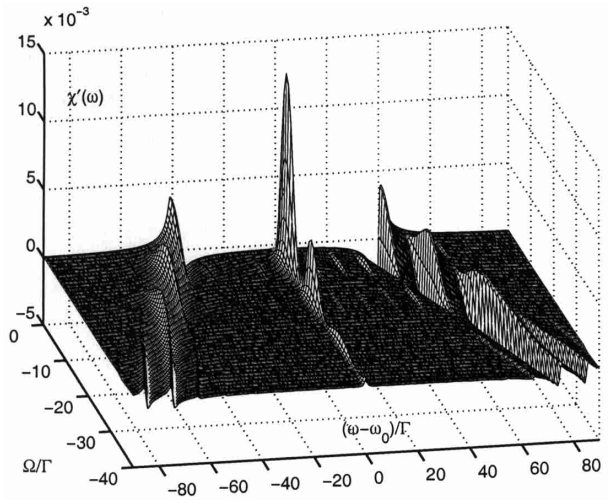

Fig. 2. Same as in Figure 1, but with $\phi_n = \pi$.

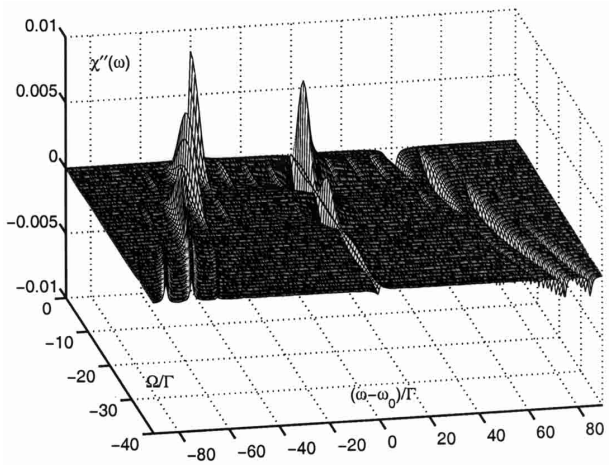

Fig. 3. Three-dimensional dispersive spectra $\chi''(\omega)$ as a function of $(\omega - \omega_0)/\Gamma$ and Ω/Γ for $\Omega_0 = 40\Gamma, \delta = 10\Gamma, p = 25$, and $\phi_n = \pi$.

starts to build up rapidly as Ω increases and attains a prompt maximum at $\Omega = \delta/2$. The amplitude of the central peak oscillates with Ω and, in contrast to the case of $\phi_n = 0$, decreases with increasing Ω. In spite of the increase of the number of resonance frequencies, the spectrum also shows an interesting stabilisation of the number of frequencies at which the system responses to the probe field. When the Rabi frequency of the modulating fields increases the system, initially responding at two frequencies, begins responding at a large number of frequencies located at multiples of $\pm\delta$. In this case, there is a large number of frequencies at which the system is transparent for the probe field. Thus, this case illustrates an interesting example for the occurrence of multiple electromagnetically induced transparency. In addition, there are broad regions in which $\chi'(\omega)$ is negative, corresponding to probe-field amplification. When $\Omega = \delta$, the multi-frequency response reduces to only two frequencies, which is similar to that observed for $\Omega = 0$, but of larger frequency separations. When Ω is increased to $3\delta/2$, the response of the system again breaks up into multiple frequencies. Thus, the multi-field dressing, seen for $\Omega = (n + 1/2)\delta$, reduces to a monochromatic (single field) dressing when $\Omega = n\delta$. This behavior may make this system useful as a quantum frequency filter.

The stabilisation of the response of the system to a probe field is better seen in the dispersion spectrum. In Figure 3, we show the dispersion spectrum $\chi''(\omega)$ for the same parameters as in Figure 2. The spectrum exhibits a large positive dispersion at the lower-frequency sidebands and a negative dispersion at the higher-frequency sidebands. The peaks of $\chi''(\omega)$ occur at exactly the frequencies at which $\chi'(\omega)$ vanishes. Moreover, for $\Omega = (n+1/2)\delta$ there is a steep normal dispersion at $\nu = 0$. The dispersion at $\nu = 0$ oscillates with Ω and its amplitude decreases with increasing Ω and becomes less steep.

The degree of the oscillatory behavior of the central absorptive and dispersive peaks and the process of undressing the atom are sensitive function of the modulation frequency δ. This is shown in Figure 4, where we plot the

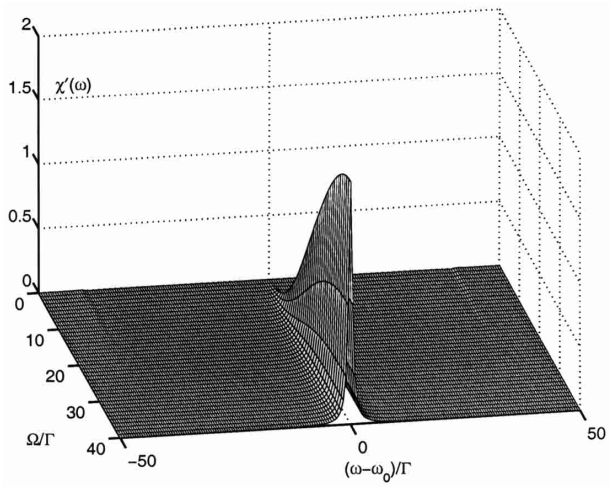

Fig. 4. Three-dimensional absorption spectra $\chi'(\omega)$ as a function of $(\omega - \omega_0)/\Gamma$ and Ω/Γ for $\Omega_0 = 40\Gamma, \delta = 40\Gamma, p = 25$, and $\phi_n = 0$.

absorption spectrum for the same parameters as in Figure 1, but $\delta = \Omega_0 = 40\Gamma$. Instead of jumping between different resonance frequencies, the sideband features located at $\pm\delta$ do not move towards the central component when Ω increases. The positions of the features remain constant, but their amplitudes vanish when $\Omega = \Omega_0$. Moreover, the central peak builds up without oscillations and, similar to Figure 1, attains maximum value at $\Omega = \Omega_0$.

Further interesting behavior is illustrated in Figure 5, where we plot the absorption spectrum for the same parameters as in Figure 4, but with $\Omega \to -\Omega$. Here, the dispersive features at $\pm\Omega_0$ decay exponentially with an increasing Ω and simultaneously dispersive features build up at $\pm 2\Omega_0$. In addition, at the point $\Omega = \Omega_0/2$, where both the sidebands have the same amplitudes, a large central (absorptive) peak appears in the spectrum. Thus, the transfer of the response of the system from the sideband frequencies $\pm\Omega_0$ to frequencies $\pm 2\Omega_0$ appears through a stabilisation of the atom in its ground state.

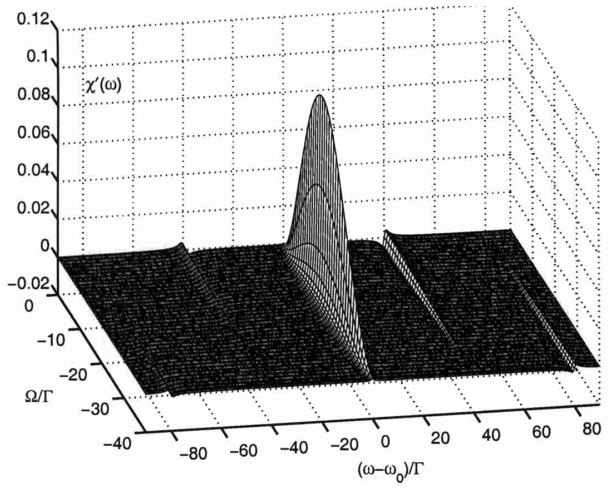

Fig. 5. Same as in Figure 4, but with $\phi_n = \pi$.

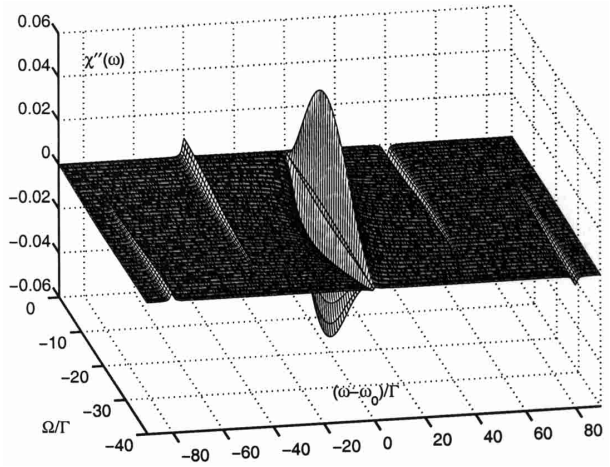

Fig. 6. Three-dimensional dispersive spectra $\chi''(\omega)$ as a function of $(\omega - \omega_0)/\Gamma$ and Ω/Γ for $\Omega_0 = 40\Gamma, \delta = 40\Gamma, p = 25$, and $\phi_n = \pi$.

Figure 6 exhibits the effect of the multiple-modulation on the dispersion spectrum for the same parameters as in Figure 5. When the Rabi frequency of the modulating field increases the positive (negative) dispersion switches from the frequency $\Omega_0(-\Omega_0)$ to $2\Omega_0(-2\Omega_0)$. The switching process is accompanied by a steep normal dispersion appearing at the central frequency for $\Omega = \Omega_0/2$. However, the steep dispersion is accompanied by an absorption (see Fig. 5).

3 Analytical results

The physics associated with the unusual response of the multiple driven two-level atom to a probe field can be understood more intuitively by approximate analytical solutions. Proceeding in a manner identical to that we calculated the fluorescence spectrum of a two-level atom driven by a multiple modulated field [11], we introduce linear combinations of the two-time components $\chi_i(t,t')$ as

$$\begin{aligned} V(t,t') &= \frac{1}{2}\left(\chi_1(t,t') - \chi_2(t,t')\right), \\ U(t,t') &= \chi_3(t,t') + \frac{\mathrm{i}}{2}\left(\chi_1(t,t') + \chi_2(t,t')\right), \\ W(t,t') &= \chi_3(t,t') - \frac{\mathrm{i}}{2}\left(\chi_1(t,t') + \chi_2(t,t')\right), \end{aligned} \quad (22)$$

where $\chi_k(t,t')$ are defined in equation (11).

Following the method of reference [11], we find that the time dependence of $V(t,t')$ has the simple exponential form

$$V(t,t') = V(t',t')\,\mathrm{e}^{-\frac{1}{2}\Gamma\left(t-t'\right)}, \quad (23)$$

where $V(t',t')$ is the initial value of $V(t,t')$.

Under the secular approximation, the time dependence of the remaining components $U(t,t')$ and $W(t,t')$, is given by

$$\begin{aligned} U(t,t') &= U(t',t') \\ &\quad \times \mathrm{e}^{-\left(\frac{3}{4}\Gamma - \mathrm{i}\Omega_0\right)\left(t-t'\right) - \mathrm{i}\sum_n A_n\left(\sin n\delta t' - \sin n\delta t\right)}, \\ W(t,t') &= W(t',t') \\ &\quad \times \mathrm{e}^{-\left(\frac{3}{4}\Gamma + \mathrm{i}\Omega_0\right)\left(t-t'\right) + \mathrm{i}\sum_n A_n\left(\sin n\delta t' - \sin n\delta t\right)}, \end{aligned} \quad (24)$$

where $A_n = 2\Omega_n/(n\delta)$.

The solutions (23, 24) allow to reproduce the different components found in the absorption and dispersion spectra by the numerical analysis and to derive approximate expressions for their intensities and widths. By decomposing the sine oscillating terms, appearing in equation (24), into Fourier components [21]

$$\begin{aligned} \mathrm{e}^{\pm \mathrm{i}A_n \sin n\delta t'} &= \sum_{q_n} J_{q_n}(\pm A_n)\,\mathrm{e}^{\mathrm{i}q_n n\delta t'}, \\ \mathrm{e}^{\pm \mathrm{i}A_n \sin n\delta t} &= \sum_{r_n} J_{r_n}(\pm A_n)\,\mathrm{e}^{\mathrm{i}r_n n\delta t}, \end{aligned} \quad (25)$$

where $J_{q_n}(A_n)$ is the q_nth order Bessel function, the solutions (24) become

$$\begin{aligned} U(t,t') &= U(t',t') \sum_{q_1,r_1} \cdots \sum_{q_p,r_p} J_{q_1}(A_1)\,J_{r_1}(-A_1)\,J_{q_2}(A_2) \\ &\quad \times J_{r_2}(-A_2) \ldots J_{q_p}(A_p)\,J_{r_p}(-A_p) \\ &\quad \times \mathrm{e}^{-\left[\frac{3}{4}\Gamma - \mathrm{i}\left(\Omega_0 + \sum_n n q_n \delta\right)\right]\left(t-t'\right)} \mathrm{e}^{-\mathrm{i}\sum_n (q_n + r_n) n\delta t}, \\ W(t,t') &= W(t',t') \sum_{q_1,r_1} \cdots \sum_{q_p,r_p} J_{q_1}(A_1)\,J_{r_1}(-A_1)\,J_{q_2}(A_2) \\ &\quad \times J_{r_2}(-A_2) \ldots J_{q_p}(A_p)\,J_{r_p}(-A_p) \\ &\quad \times \mathrm{e}^{-\left[\frac{3}{4}\Gamma + \mathrm{i}\left(\Omega_0 + \sum_n n q_n \delta\right)\right]\left(t-t'\right)} \mathrm{e}^{+\mathrm{i}\sum_n (q_n + r_n) n\delta t}. \end{aligned} \quad (26)$$

Equation (26) shows that an nth pair of the sideband fields is equivalent to a resonant field with an amplitude of

$J_0(A_n)$ plus nonresonant fields at the detuned frequencies $nq_n\delta$ and amplitudes $J_{q_n}(A_n)$.

According to the definition of the susceptibility (10), we have to evaluate the two-time correlation function of the atomic dipole operators. With the help of equation (22), one finds that the two-time correlation function can be expressed by the linear combinations V, U and W as

$$\chi_1(t,t') = V(t,t') - \frac{\mathrm{i}}{2}\left(U(t,t') - W(t,t')\right). \quad (27)$$

Hence, in the secular approximation, the absorption and dispersion spectra are given by

$$\chi'(\omega)/\Gamma = -\frac{1}{2}\frac{X_3^{(0)}\Gamma}{\left(\frac{\Gamma}{2}\right)^2+\nu^2} + \frac{1}{2}\tilde{X}_2^{(0)}\sum_{q_1,r_1}\cdots\sum_{q_p,r_p} \times\left\{\frac{J_{q_1}(A_1)J_{r_1}(-A_1)\ldots J_{q_p}(A_p)J_{r_p}(-A_p)(\nu+D)}{\frac{9}{16}\Gamma^2+(\nu+D)^2} \times\delta_{q_1+r_1+\ldots+pq_p+pr_p,0} + \frac{J_{q_1}(A_1)J_{r_1}(-A_1)\ldots J_{q_p}(A_p)J_{r_p}(-A_p)(\nu-D)}{\frac{9}{16}\Gamma^2+(\nu-D)^2} \times\delta_{q_1+r_1+\ldots+pq_p+pr_p,0}\right\}, \quad (28)$$

and

$$\chi''(\omega)/\Gamma = -\frac{X_3^{(0)}\nu}{\left(\frac{\Gamma}{2}\right)^2+\nu^2} + \frac{3}{4}\tilde{X}_2^{(0)}\sum_{q_1,r_1}\cdots\sum_{q_p,r_p} \times\left\{\frac{J_{q_1}(A_1)J_{r_1}(-A_1)\ldots J_{q_p}(A_p)J_{r_p}(-A_p)\Gamma}{\frac{9}{16}\Gamma^2+(\nu+D)^2} \times\delta_{q_1+r_1+\ldots+pq_p+pr_p,0} + \frac{J_{q_1}(A_1)J_{r_1}(-A_1)\ldots J_{q_p}(A_p)J_{r_p}(-A_p)\Gamma}{\frac{9}{16}\Gamma^2+(\nu-D)^2} \times\delta_{q_1+r_1+\ldots+pq_p+pr_p,0}\right\}, \quad (29)$$

where $D = \Omega_0 + \sum_n nq_n\delta$, and $\tilde{X}_2^{(0)} = \mathrm{Im}X_2^{(0)}$.

It is seen from equations (28, 29) that the sideband features of the spectra are located at multiplets of δ and their positions are independent of the number of modulating fields and their Rabi frequencies. However, the amplitudes of the sideband features depend on the number of modulating fields and their Rabi frequencies. Moreover, the dependence of the amplitudes on the Kronecker delta function indicates that only these terms contribute to the spectrum for which

$$q_1 + r_1 + 2q_2 + 2r_2 + \ldots + pq_p + pr_p = 0. \quad (30)$$

There is an infinite number of the parameters q_n and r_n satisfying the condition (30). The spectra (28, 29) have complicated structures and it is difficult to predict the behavior of the spectra on the number of modulating fields. However, in our numerical calculations of Section 2, we assumed that the driving field is composed of a large number of frequency components ($p \gg 1$). In this case, we can approximate the sums appearing in equation (24) by [21,22]

$$\sum_n A_n\left(\sin n\delta t' - \sin n\delta t\right) \approx \Omega t - \Omega t'. \quad (31)$$

Hence, in the limit of $p \gg 1$, the absorption and dispersion spectra can be written as

$$\chi'(\omega) = \frac{1}{2}\Gamma\left\{-X_3^{(0)}\frac{\Gamma}{\frac{1}{4}\Gamma^2+\nu^2} + \tilde{X}_2^{(0)}\frac{(\nu+\Omega_0-\Omega)}{\frac{9}{16}\Gamma^2+(\nu+\Omega_0-\Omega)^2} + \tilde{X}_2^{(0)}\frac{(\nu-\Omega_0+\Omega)}{\frac{9}{16}\Gamma^2+(\nu-\Omega_0+\Omega)^2}\right\}, \quad (32)$$

and

$$\chi''(\omega) = \frac{1}{2}\Gamma\left\{-2X_3^{(0)}\frac{\nu}{\frac{1}{4}\Gamma^2+\nu^2} + \frac{3}{4}\tilde{X}_2^{(0)}\frac{\Gamma}{\frac{9}{16}\Gamma^2+(\nu+\Omega_0-\Omega)^2} + \frac{3}{4}\tilde{X}_2^{(0)}\frac{\Gamma}{\frac{9}{16}\Gamma^2+(\nu-\Omega_0+\Omega)^2}\right\}. \quad (33)$$

It is clear from equations (32, 33) that the "effective" Rabi frequency of a multiple modulated field is equal to the difference $\Omega_0 - \Omega$ and vanishes for $\Omega = \Omega_0$. As a result, the Rabi sidebands of the spectrum move towards the central component as Ω increases and disappear for $\Omega = \Omega_0$. When we change the phase of the modulating fields, $\Omega \to -\Omega$, and then the effective Rabi frequency changes to $\Omega_0 + \Omega$. In this case, the sidebands move away from the central component as Ω increases.

It is seen from equation (32) that the magnitude of the central component of the absorption spectrum depends on the stationary component of the inversion $X_3^{(0)}$, whereas the sideband features depend on the imaginary part of the dipole moment $X_2^{(0)}$. We have checked numerically that $\tilde{X}_2^{(0)}$ is very small independent of Ω. On the other hand, the inversion can be reduced at some Ω and may even reach the maximum negative value $X_3^{(0)} = -1/2$. This is shown in Figure 7, where we plot the population inversion $X_3^{(0)}$ as a function of Ω for the same parameters as in Figure 1. Clearly, the inversion oscillates with Ω and at $\Omega = \Omega_0$, $X_3^{(0)} \approx -1/2$ showing that at $\Omega = \Omega_0$ the atom collapses into its ground state. This fact clearly explains the appearance of a large absorptive peak in the absorption spectrum and the disappearance of the Rabi sidebands. In Figure 8, we plot the population inversion for the same parameters as in Figure 4.

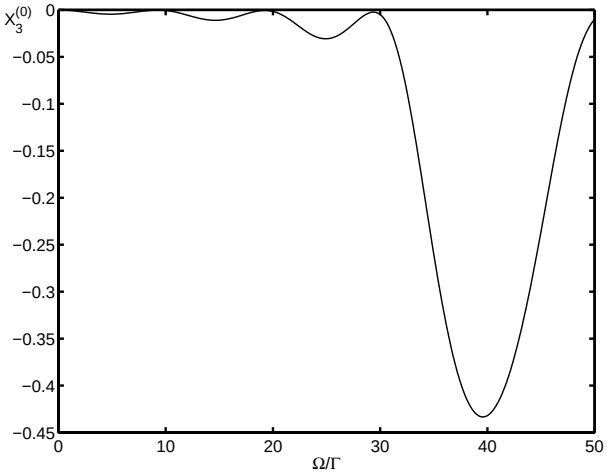

Fig. 7. The steady-state population inversion $X_3^{(0)}$ as a function of Ω for $\Omega_0 = 40\Gamma, \delta = 10\Gamma, p = 25$ and $\phi_n = 0$.

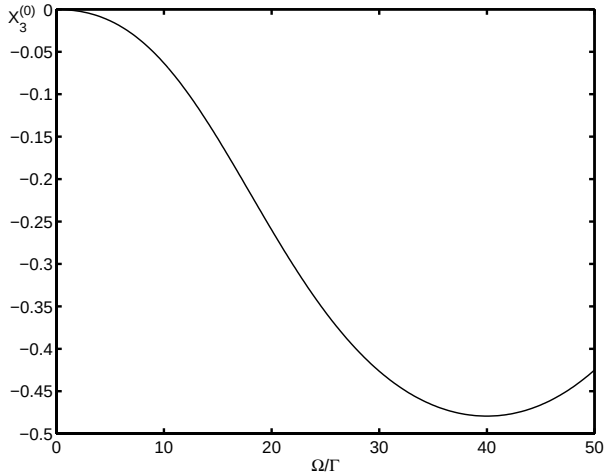

Fig. 8. Same as in Figure 7, but with $\delta = 40\Gamma$.

In this case the population inversion monotonically evolves towards $X_3^{(0)} = -1/2$, that clearly explains the nonoscillatory increase of the absorption at the central frequency, seen in Figure 4.

4 Summary

We have presented a detailed analysis of the probe absorption and dispersion spectra of a two-level atom driven by a multiple-modulated field. We have calculated the spectrum numerically using a Floquet approach and have explained the spectral features calculating analytically the spectrum in terms of the Bessel functions. We have shown that in the limit of a large frequency components of the modulating field the spectral features are very sensitive to the Rabi frequency and initial phase of the modulating field. For the initial phases equal to zero, the dispersive features located at the sideband frequencies move towards the central component as the Rabi frequency of the modulating field increases, and an absorption peak emerges at the central frequency whose the amplitude increases in an oscillatory manner. The continuous move of the sideband features towards the central component and the appearance of a strong absorption peak at the central frequency clearly demonstrate that the multiple-modulated field returns the atom to its ground state. The absorption and dispersion spectra reflect the dressing properties of a strong driving field, or equivalently the entanglement of atomic and driving field states. Hence, the predicted spectra offer a method of observing undressing and disentanglement by a multiple-modulated field. Moreover, we have shown an interesting effect of stabilisation of the frequencies at which the driven two-level atom responses to the probe field, that could make this system useful as a quantum frequency filter.

This work has been supported by the Jubiläumsfonds der Oesterreichischen Nationalbank zur Förderung der Forschungs- und Lehraufgaben der Wissenschaft under Contract No. 7720. A.V.S. and N.N.B. acknowledge support from the RFBR program of Support for Leading Scientific Schools, Grant No. 00-15-96149 and would also like to thank the Österreichische Akademie der Wissenschaften for the invitation and support of the visit to the Institut für Theoretische Physik, Technische Universität Wien.

References

1. M.O. Scully, M. Fleischhauer, Phys. Rev. Lett. **69**, 1360 (1992); H. Freedhoff, T. Quang, J. Opt. Soc. Am. B **12**, 9 (1995); D. Bortman-Arbiv, A.D. Wilson-Gordon, H. Friedmann, Phys. Rev. A **63**, 043818 (2001).
2. A.M. Akulshin, S. Barreiro, A. Lezama, Phys. Rev. Lett. **83**, 4277 (1999); M. Artoni, G.C. La Rocca, F.S. Cataliotti, F. Bassani, Phys. Rev. A **63**, 023805 (2001).
3. S.E. Harris, Phys. Rev. Lett. **62**, 1033 (1989); for a recent review see E. Arimondo, in *Progress in Optics XXXV*, edited by E. Wolf (Elsevier, Amsterdam, 1996), p. 257.
4. A.D. Wilson-Gordon, H. Friedmann, Opt. Commun. **94**, 238 (1992); H. Freedhoff, T. Quang, Phys. Rev. A **48**, 3216 (1993); C. Szymanowski, C.H. Keitel, B.J. Dalton, P.L. Knight, J. Mod. Opt. **42**, 985 (1995); M.R.B. Wahiddin, Z. Ficek, U. Akram, K.T. Lim, M.R. Muhamad, Phys. Rev. A **57**, 2072 (1998); R.S. Bennink, R.W. Boyd, C.R. Stroud Jr, V. Wong, Phys. Rev. A **63**, 033804 (2001).
5. M.O. Scully, Phys. Rev. Lett. **67**, 1855 (1991); M. Fleischhauer, C.H. Keitel, M.O. Scully, C. Su, B.T. Ulrich, S.-Y. Zhu, Phys. Rev. A **46**, 1468 (1992); S.E. Harris, J.E. Field, A. Kasapi, Phys. Rev. A **46**, R29 (1992).
6. B.R. Mollow, Phys. Rev. A **5**, 1522, 2217 (1972).
7. F.Y. Wu, S. Ezekiel, M. Ducloy, B.R. Mollow, Phys. Rev. Lett. **38**, 1077 (1977).
8. Ph. Tamarat, F. Jelezko, Ch. Brunel, A. Maali, B. Lounis, M. Orrit, Chem. Phys. **245**, 121 (1999), and references therein.
9. For a review on the strong probe spectroscopy see Z. Ficek, H.S. Freedhoff, in *Progress in Optics XL*, edited by E. Wolf (Elsevier, Amsterdam, 2000), p. 389.
10. C. Cohen-Tannoudji, S. Reynaud, J. Phys. B **10**, 345 (1977); C. Cohen-Tannoudji, J. Dupont-Roc, G. Grynberg, *Atom-Photon Interactions* (Wiley, New York, 1992).

11. Z. Ficek, J. Seke, A.V. Soldatov, G. Adam, J. Opt. B: Quant. Semiclass. Opt. **2**, 780 (2000); Phys. Rev. A **64**, 013813 (2001).
12. M.H. Mittleman, Phys. Rev. A **32**, 276 (1985).
13. Y. Zhu, A. Lezama, D.J. Gauthier, T.W. Mossberg, Phys. Rev. A **41**, 6574 (1990); Q. Wu, D.J. Gauthier, T.W. Mossberg, Phys. Rev. A **49**, R1519 (1994); Q. Wu, D.J. Gauthier, T.W. Mossberg, Phys. Rev. A **50**, 1474 (1994); C.C. Yu, J.R. Bochinski, T.M.V. Kordich, T.W. Mossberg, Z. Ficek, Phys. Rev. A **56**, R4381 (1997); J.R. Bochinski, C.C. Yu, T. Loftus, T.W. Mossberg, Phys. Rev. A **63**, 051402(R) (2001).
14. H. Carmichael, *An Open Systems Approach to Quantum Optics*, Lecture Notes in Physics (Springer-Verlag, Berlin, 1993), p. 45.
15. Yu.A. Zinin, N.V. Sushilov, Phys. Rev. A **51**, 3916 (1995); T.H. Yoon, S.A. Pulkin, J.R. Park, M.S. Chung, H.-W. Lee, Phys. Rev. A **60**, 605 (1999); T.H. Yoon, M.S. Chung, H.-W. Lee, Phys. Rev. A **60**, 2547 (1999).
16. J.H. Eberly, K. Wódkiewicz, J. Opt. Soc. Am. **67**, 1252 (1977).
17. N. Lu, P.R. Berman, A.G. Yodh, Y.S. Bai, T.W. Mossberg, Phys. Rev. A **33**, 3956 (1986).
18. M. Lax, Phys. Rev. **129**, 2342 (1963); Phys. Rev. **157**, 213 (1967).
19. S. Stenholm, *Foundations of Laser Spectroscopy* (Wiley, New York, 1984); S.I. Chu, Adv. At. Mol. Phys. **21**, 197 (1985).
20. B. Blind, P.R. Fontana, P. Thomann, J. Phys. B **13**, 2717 (1980).
21. M. Abramowitz, I. Stegun, *Handbook of Mathematical Functions* (Dover, New York, 1972), p. 361.
22. I.S. Gradshteyn, I.M. Ryzhik, *Table of Integrals, Series, and Products* (Academic Press, New York, 1965), p. 38.